Supporting Information for

Facile Solvothermal Synthesis of MIL-47(V) Metal-Organic Framework for a High-Performance Epoxy/MOF Coating with Improved Anticorrosion Properties

Mahmoud Y. Zorainy,[a,b] Mohamed Sheashea,[b] Serge Kaliaguine,[c] Mohamed Gobara,[b] and Daria. C. Boffito[a]*

[a] *Chemical Engineering Department, Polytechnique Montréal, Montréal, QC H3C 3A7 (Canada)*
[b] *Chemical Engineering Department, Military Technical College, Cairo (Egypt)*
[c] *Chemical Engineering Department, Laval University, Québec, QC G1V 0A6 (Canada)*
**Corresponding Author: daria-camilla.boffito@polymtl.ca*

Table of Content **Page no.**

1. Experimental details

1.1 Materials.

Vanadium(V) oxide (V_2O_5, ≥ 98%), 1,4-Benzene dicarboxylic acid "terephthalic acid" (H_2BDC or TPA, 98%), and *N*, *N*-dimethyl formamide (anhydrous DMF, 99.8%) were used to synthesize the MIL-47(V)as framework. They were all purchased from Sigma-Aldrich, Canada. Ethanol (EtOH, 98%) was purchased from Fischer Scientific, USA, and was applied in the washing and activation process.

Diglycidyl ether of bisphenol A, commonly known as Epoxy or component A, with an equivalent weight of 450–500 g/equiv. (Huntsman, China) was applied as the main coating. Diethylenetriamine (DETA), a tertiary amine acting as a curing agent or hardener (component B), was purchased from CDH, India. Acetone as the coating thinner, in addition to sodium chloride (NaCl, ≥ 99.0%) for the corrosive medium preparation, were purchased from Sigma-Aldrich, Canada.

All chemicals were used as received with no further processing, and all aqueous solutions were prepared with deionized water. All experimental procedures were performed under ambient atmosphere unless otherwise stated.

1.2 Methods.

- Synthesis of MIL-47(V) metal-organic framework:

The MIL-47(V) metal-organic framework was solvothermally-synthesized in a Parr's 200-ml large capacity acid digestion vessel (Parr Instrument Company, Model# 4748A) to provide a sufficient amount of MOF for all experiments, ensuring that all samples are the same. In a typical procedure, a 1:1 metal-to-linker ratio mixture was prepared, whereby 4.55 g V_2O_5 (25 mmol) and 4.15 g H_2BDC (25 mmol) were weighed, mixed, and dissolved in a 100 ml DMF (Figure S1-A). The mixture was then stirred for 30 min. Since V_2O_5 is not completely soluble in DMF, a bright-orange colored slurry of a pH around 5.3 was formed (Figure S1-B). Next, the slurry was transferred into the Teflon-lined autoclave bomb and heated to 180 °C in a conduction oven. The reaction was held at this temperature for 20 h without stirring. The bomb was then left to cool down gradually to room temperature inside the oven.

The reaction yielded a deep green colored suspension of a pH around 7.7 (Figure S1-C). Powders of a greenish-yellow color were collected through centrifugation at a speed of 10,000 rpm for 10 min (MIL-47as, Figure S1-D).[1] The separated solids were thoroughly washed with DMF (×3) and ethanol (×3). After each wash, the powders were rinsed and vortexed for 1 min at 3000 rpm. The as-synthesized product (MIL-47as) was thermally activated at 300 °C for 12 h to remove any unreacted BDC linker within the pores, yielding the oxidized non-flexible form (MIL-47) of a yellow color (Figure S1-E).[2]

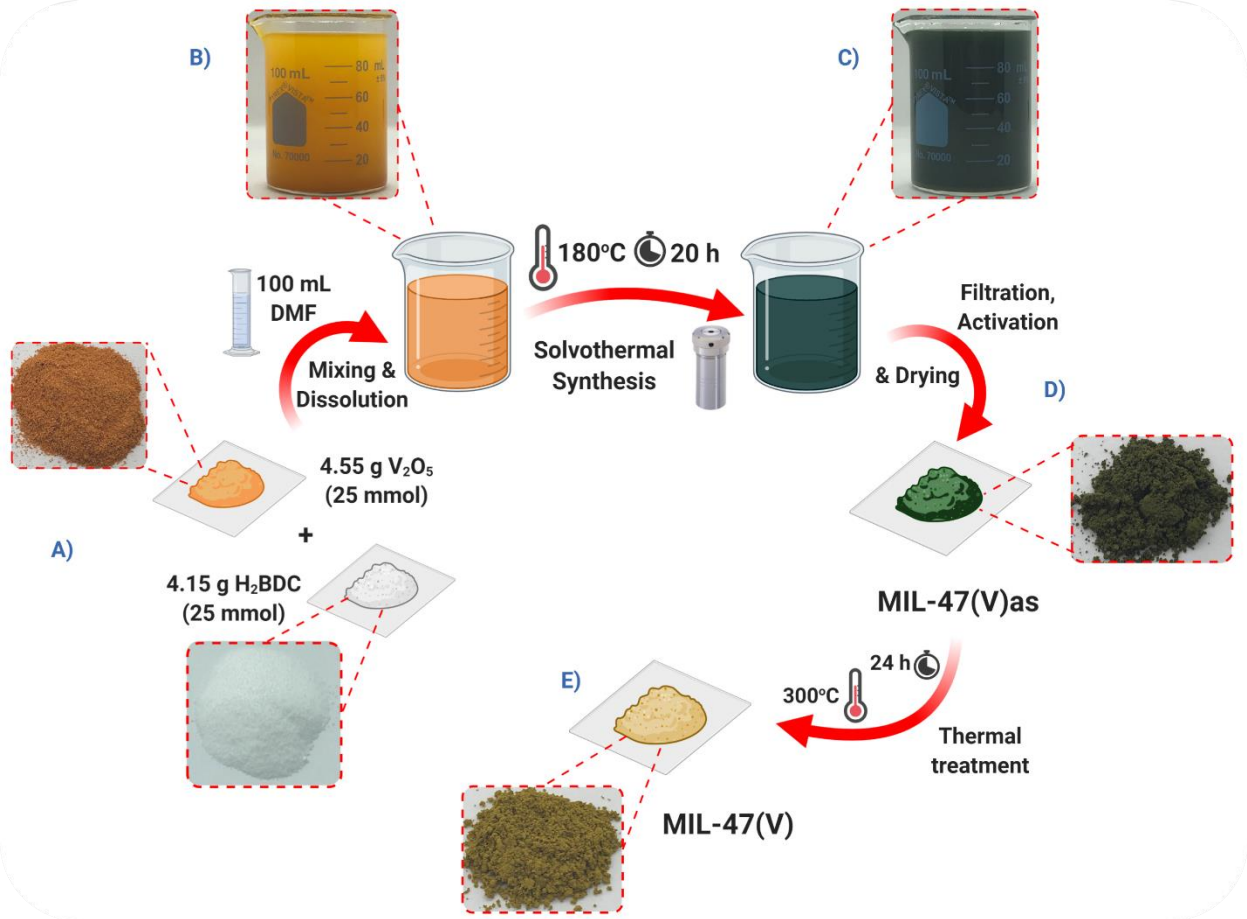

Figure S1. The solvothermal synthesis of the MIL-47 metal-organic framework. A) Mixing of the metal and organic precursors, B) Orange slurry before synthesis, C) Deep-green suspension after synthesis, D) Greenish-yellow powder of as-synthesized MIL-47 "MIL-47as", E) MIL-47 as a final product after thermal activation.

- Aluminum alloy specimen, epoxy coating, and corrosive medium preparation:

Aluminum alloy AA2024, Cu-rich as the main alloying component, was employed as the working electrode Rectangular-shaped coupons with dimensions of [L×W×H= 12.5 cm × 2.5 cm × 0.1 cm] and a typical composition of wt.%: Cu(3.8-4.9), Mg(1.2-1.8), Si(0.50), Fe(0.50), Mn(0.3-0.9), Cr(0.10), Zn(0.25), Ti(0.15), and Al(balance) were obtained from Q-panel™, USA. The surface of the coupons was sanded with 320, 600, and 1200 grit abrasive SiC paper to remove the outer layer containing any scale or contamination and prepare the metal surface for the next step of coating. These coupons were then cleaned with ethanol, followed by deionized water before drying at room temperature through a compressed air stream for 1 min. After drying, the coupons were stored in a dry environment, desiccator with silica gel, until use in the corrosion evaluation experiments.

For comparison, a neat epoxy coating was prepared side-by-side to the MOF/epoxy one. The preparation of the neat epoxy included the following steps: 2 g of component A (untreated epoxy resin) was weighed and dissolved in 5 ml acetone. Then, the solution was stirred for 5 min until the complete dissolution of the resin. An equivalent amount of the DETA hardener (component B) was then added to the solution and left to stir in a closed flask for another 5 min at room temperature. For the MOF/epoxy coating, 0.2 g of the as-synthesized MOF (MIL-47as) was sonicated with the epoxy solution for 5 min using an ultrasonic probe homogenizer (400 W - 24 kHz, 50% Amp., Hielscher - Germany), before adding the hardener. Finally, the obtained solution was applied to the aluminum coupons through spray coating using an airbrush to obtain a uniform coat with a thickness of 10 ± 2 μm. The samples were cured in a clean room for 36 h, followed by placing in a conduction oven at 60°C overnight.

An aqueous solution of 3.5 wt.% NaCl was prepared to simulate the artificial seawater corrosive medium and the chloride-rich environment. Such an aggressive electrolyte is able to destroy the superficial passive aluminum oxide layer and develop a localized corrosion attack. This solution is the standard corrosive electrolyte for the AA2xxx series in corrosion evaluation standards, like ASTM G44 and G47.

2. Characterization.

2.1 General Characterization:

Powder X-ray diffraction (PXRD) patterns were recorded on a Bruker D8 Advance X-ray diffractometer equipped with LYNXEYE linear position-sensitive detector (Bruker AXS, Madison, WI). Data was collected over a 2θ-range of 3 ° - 50 ° at an increment of 0.02 ° and a scanning rate of 0.2 ° s^{-1}. The diffractometer, with a Cu-K_α source (λ = 1.5406 Å), operated at a tube voltage and current of 40 kV and 40 mA, respectively. Samples for PXRD were prepared by placing a thin layer of samples on a zero-background silicon crystal plate supported on a cup.

Fourier-transform Infrared (FTIR) spectra were collected using the Perkin Elmer spectrum 65 spectrophotometer equipped with an ATR diamond. With the high-efficiency ATR technique, a full range scan (4000 cm^{-1} - 450 cm^{-1}) was performed with a resolution of 4 cm^{-1}, and the data were averaged over 32 scans.

Thermogravimetric analysis (TGA) was performed on the TA Instruments Q50 analyzer. Experiments were conducted in an oxidative flow of air (50 mL min^{-1}) in a platinum pan. Heating took place in the range of 25 ºC - 800 ºC at a rate of 10 ºC min^{-1}.

Raman spectra were obtained using a WITec alpha300R access confocal Raman microscope equipped with a motorized stage, CCD detector, and 1800 grooves mm^{-1} optical grating. In addition, the instrument was equipped with a green cobalt laser source of a 532 nm wavelength. Measurements were done using three collecting lenses (10x, 50x, and 100x). Powder samples were first pressed against a glass microscope slide. Spot analysis was then adopted over some selected

spots in each sample with an accumulating response of 20 scans, each of a signal integration time of 10 s to ensure that the obtained MOF is free from any metal oxide phases. Spectra were collected in the region from 100 cm^{-1} to 3500 cm^{-1}, with a resolution of 1 cm^{-1}. Area analysis over a square area of a side length of 10 µm was also recorded to get a collective response for the whole sample. Finally, the laser power was adjusted to be as low as possible to avoid any local heating induced by the laser.

A scanning electron microscope (SEM, Carl Zeiss EVO MA 10 - Germany) equipped with the energy-dispersive X-ray (EDX) detector was utilized to screen the surface structure and the compositions of all the products. Samples were dispersed on double-sided carbon tape and mounted on an aluminum stub. Mainly, the instrument was operated in the secondary electron mode to inspect the morphology of the obtained crystals at a higher magnification. The instrument was left to detect the present elements automatically and their distribution and percentage abundance with respect to the mass ratio.

2.2 Adhesion testing:

Regarding the evaluation of the coating adhesion, the crosshatch adhesion tape test (method B) was applied according to ASTM D3359. In such a test, thin crosshatch cuts were performed on the coating surface followed by the application of a standard pressure-sensitive tape to the area (ISO 2409). The tape was then removed quickly at 180°, and the surface of the coating was visually inspected under a 10x magnifying lens for the presence of any delamination occurring to the surface and on to the tape.

2.3 Electrochemical characterization studies:

The electrochemical corrosion experiments were performed at room temperature on a potentiostat/galvanostat, reference 600 Gamry™, with a standard three-electrode type cell. In all experiments, the aerated corrosive solution volume ratio to sample surface area was adjusted to be 50 ml cm^{-2}. A saturated calomel electrode was used as a reference electrode, platinum as a counter electrode, and the coated AA2024 specimen was the working electrode. The EIS tests were performed over a frequency range of 10^5 to 10^{-2} Hz with an amplitude of 10 mV peak-to-peak, using AC signal at OCP.

3. Further results.

3.1 FTIR:

Fourier-transform infrared spectroscopy (FTIR) was employed to confirm the formation of the targeted MOF and the linkage between the vanadium cations and the organic ditopic H_2BDC ligands (Figure S2). The vibrational spectrum of the obtained crystals agreed well with that reported for the MIL-47 framework, whereby the high absorption bands related to the antisymmetric and symmetric stretching of the dicarboxylate groups were easily recognized at 1533 cm^{-1} and 1394 cm^{-1}, respectively.[3] The peak at 893 cm^{-1} was assigned to the bending vibrations of the conjugated aromatic ring carbons (C=C–C), while those at 1018 cm^{-1} and 740 cm^{-1} were attributed to the in-plane stretching and out-of-plane wagging of the aromatic ring (C-H) bonds, respectively.[3]

Most importantly, the metal oxo-chains (V-O-V) vibration was detected in the far IR region around 555 cm^{-1} and 604 cm^{-1} that was ascribed to the symmetric and antisymmetric stretching, respectively.[4-6] In addition, the broad absorption around 3000 cm^{-1} confirmed the presence of OH groups within the as-synthesized MIL-47 structure, referring to a narrow-pore arrangement.[3] Moreover, the peak at 1702 cm^{-1} corresponding to protonated carboxylic groups verified the presence of unreacted linker molecules within the pores of the MOF, which is unavoidable during synthesis even after the partial pore evacuation during the washing step by DMF.[1, 7]

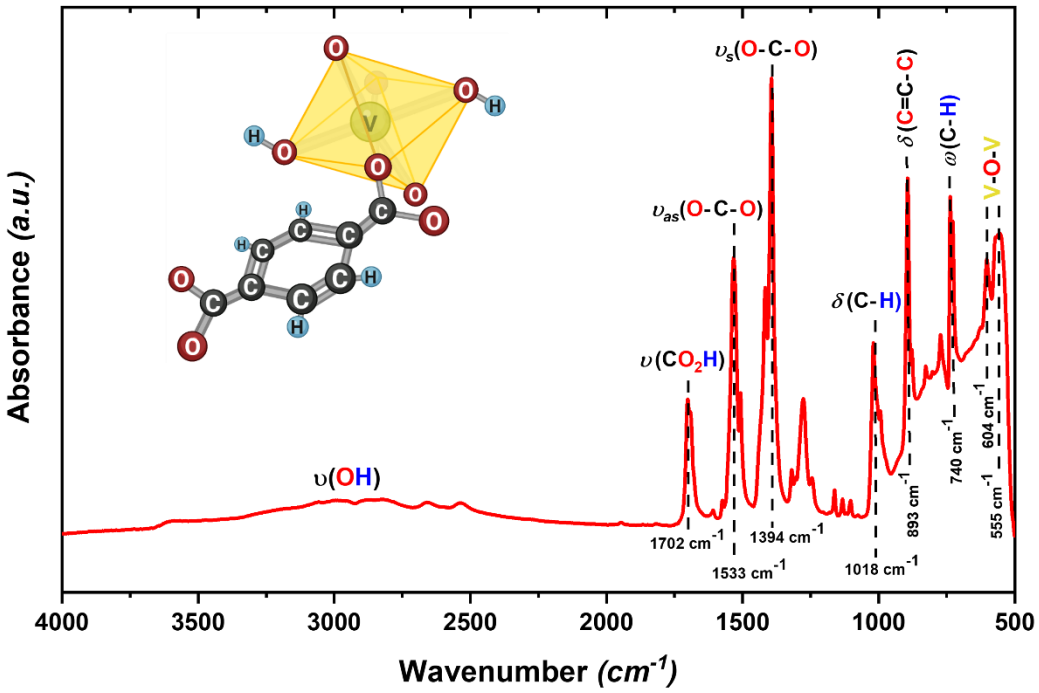

Figure S2. FTIR spectrum of the as-synthesized MIL-47 expressing the narrow-pore form and the inclusion of unreacted H_2BDC molecules within the pores. Inset: the connection of the vanadium oxo-cluster with the linker, showing different types of bonding all over the MOF structure.

3.2 Raman:

In order to ensure that the synthesized MOF is metal-oxide free, Raman spectroscopy was used as a selective technique to investigate such possible inclusion of other materials within the MOF crystals. As shown in Figure S3, actual images obtained through the instrument microscope for the vanadium pentoxide powder at different zooming levels exhibited large block-like crystals of a particle size > 50 µm and deep orange color. Raman spectra performed around these crystals recorded the characteristic vibrational bands of V_2O_5 at 151 cm^{-1}, 201 cm^{-1}, 288 cm^{-1}, 308 cm^{-1}, 412 cm^{-1}, 488 cm^{-1}, 532 cm^{-1}, 707 cm^{-1}, and 999 cm^{-1}.[6] Most importantly, the bands at 151 cm^{-1} and 201 cm^{-1} correspond to the lattice vibrations, while those at 288 cm^{-1}, 412 cm^{-1}, and 993 cm^{-1} are assigned to the vanadyl (V=O) bending and stretching vibrational modes. Also, the vibrations at 488 cm^{-1} and 707 cm^{-1} are attributed to the V-O-V bending and stretching, respectively.[8]

Investigating the powder of the as-synthesized MIL-47 framework showed greenish rod-like crystals of smaller particle size (in the range of a few microns) compared to the crystals of V_2O_5. The given spectra at different spots were alike, with the vibrational bands measured at 870 cm^{-1}, 1154 cm^{-1}, 1460 cm^{-1}, and 1622 cm^{-1} corresponding to the aromatic and dicarboxylate groups of the H_2BDC linker.[3] The bands at lower wavenumbers belong to the vibrations of the V-O chain bonds.[3, 9] The sample was screened, searching for any foreign particle, but none was found. Also, the area analysis of a large portion of the sample did not show any different signal compared to the spot analysis. Hence, we can conclude that, despite being prepared from a metal oxide precursor, the synthesis technique reported here produced pure MOF crystals without any oxide residue.

The thermally activated sample of MIL-47 showed no difference compared to the as-synthesized one, whereby the crystal had almost the same rod-like shape and average particle size. However, the MIL-47 powder appeared to have yellow color at low magnification, but the crystals seemed to be slightly greenish at higher magnification. Moreover, the recorded spectrum of MIL-47 was similar to the one of MIL-47as (Figure S3) with very minute changes. For example, in the spectrum of the thermally activated sample, the peaks related to the metal-O vibrations at lower wavenumbers were more pronounced (sharper peaks of higher intensity). In the 850 cm^{-1} - 950 cm^{-1} range, the small peak at around 891 cm^{-1} in the spectrum of MIL-47as shifted to a higher wavenumber to appear as a shoulder in the spectrum of MIL-47. On the contrary, in the 1400 cm^{-1} – 1500 cm^{-1} range, the shoulder appearing in the MIL47as spectrum around 1450 cm^{-1} was shifted to lower wavenumber in the MIL-47 spectrum. Similar shifts were noticed in the study of Yot *et al.* while studying the breathing behavior of MIL-47(V) under the effect of external mechanical forces, marking the transformations of these frameworks between different forms.[9]

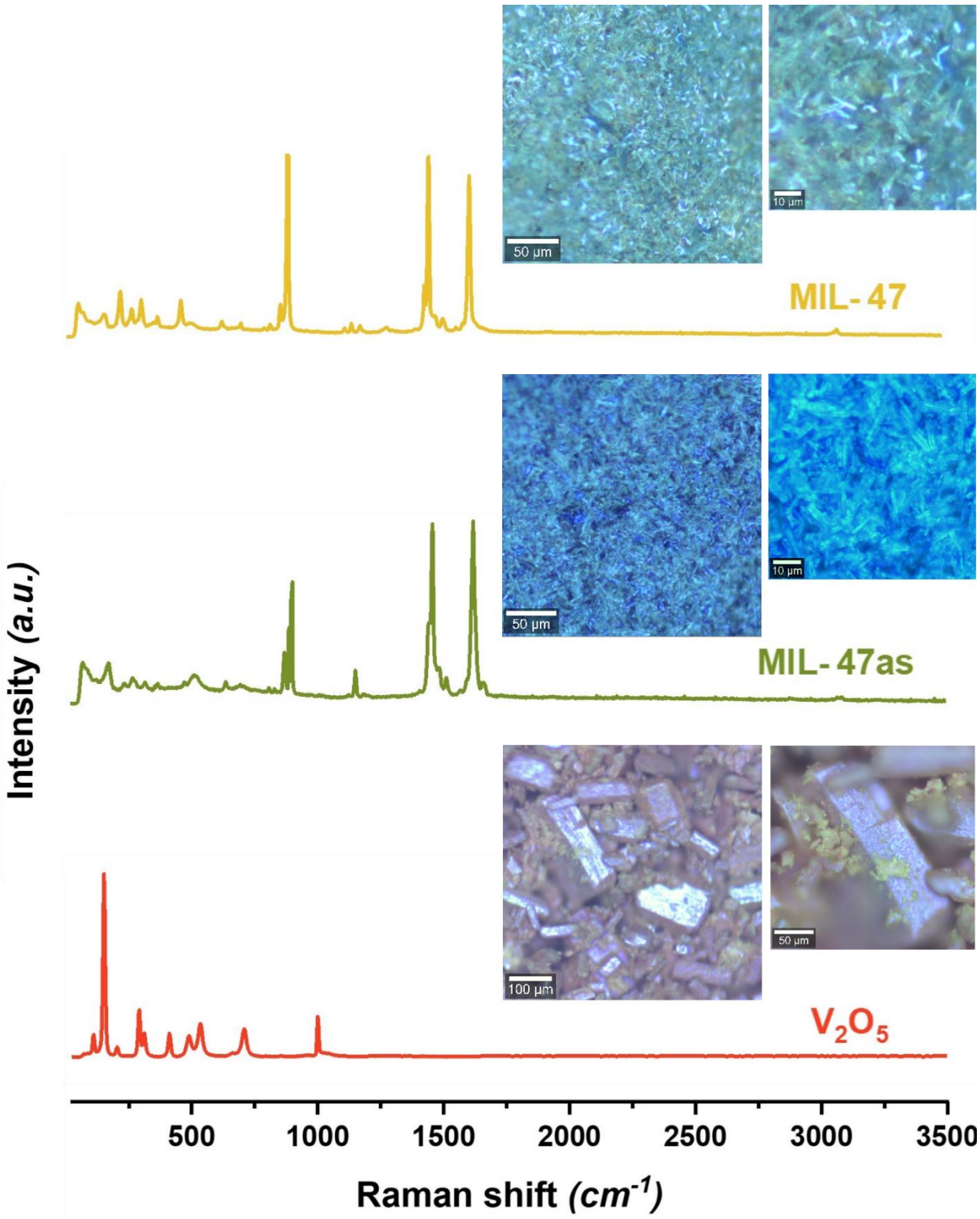

Figure S3. Raman spectra of V_2O_5 "red"; as-synthesized MIL-47 "green"; and thermally activated MIL-47 "yellow". Inset: actual optical microscopic images of the investigated spots/areas in each powder.

3.3 Coating Adhesion:

The crosshatch adhesion test was applied to both coating types (neat epoxy and MOF/epoxy) in order to evaluate their adhesion performance, both before and after immersion in the corrosive electrolyte (i.e., 3.5% NaCl solution) for 24 h. Conducting the wet adhesion was intended to assess the influence of water uptake on the adhesion properties of coatings. The crosshatch cut test of the dry samples did not show any signs of delamination after performing the test ten times on the same area, whereby the edges of the cuts were completely smooth with none of the squares detached (i.e., 5B rating). Similarly, performing the test on the wet samples was of the same results, in which the MOF/epoxy samples did not exhibit any distinguishable differences in behavior when compared to the neat epoxy ones as shown in Figure S4.

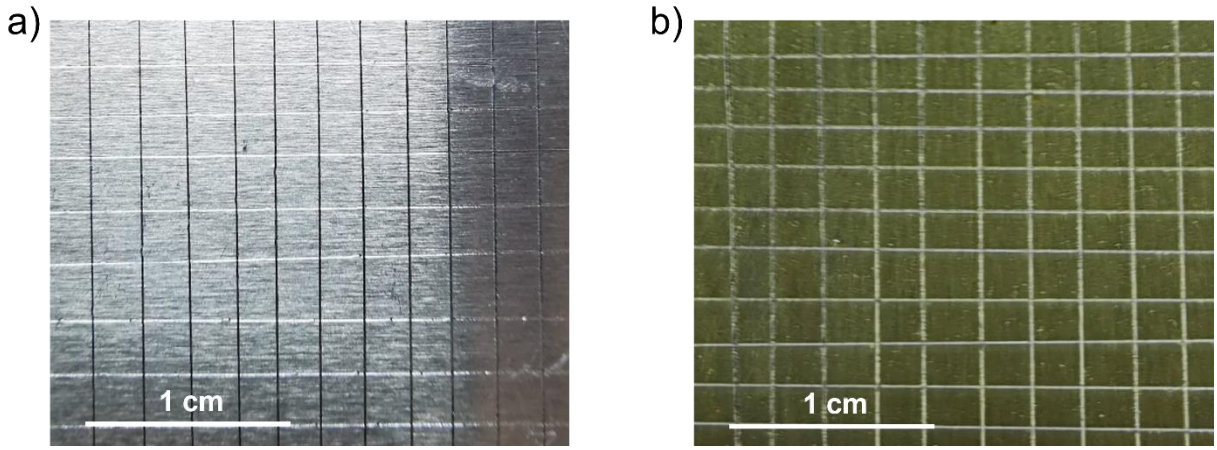

Figure S4. Adhesion test results (a) neat epoxy and (b) MOF/epoxy samples.

From these results it can be concluded that the addition of the MIL-47 MOF to the epoxy coating has not significantly changed the adhesion properties of the coating.

3.4 Corrosion performance:

- Pitting corrosion within the neat epoxy coating:

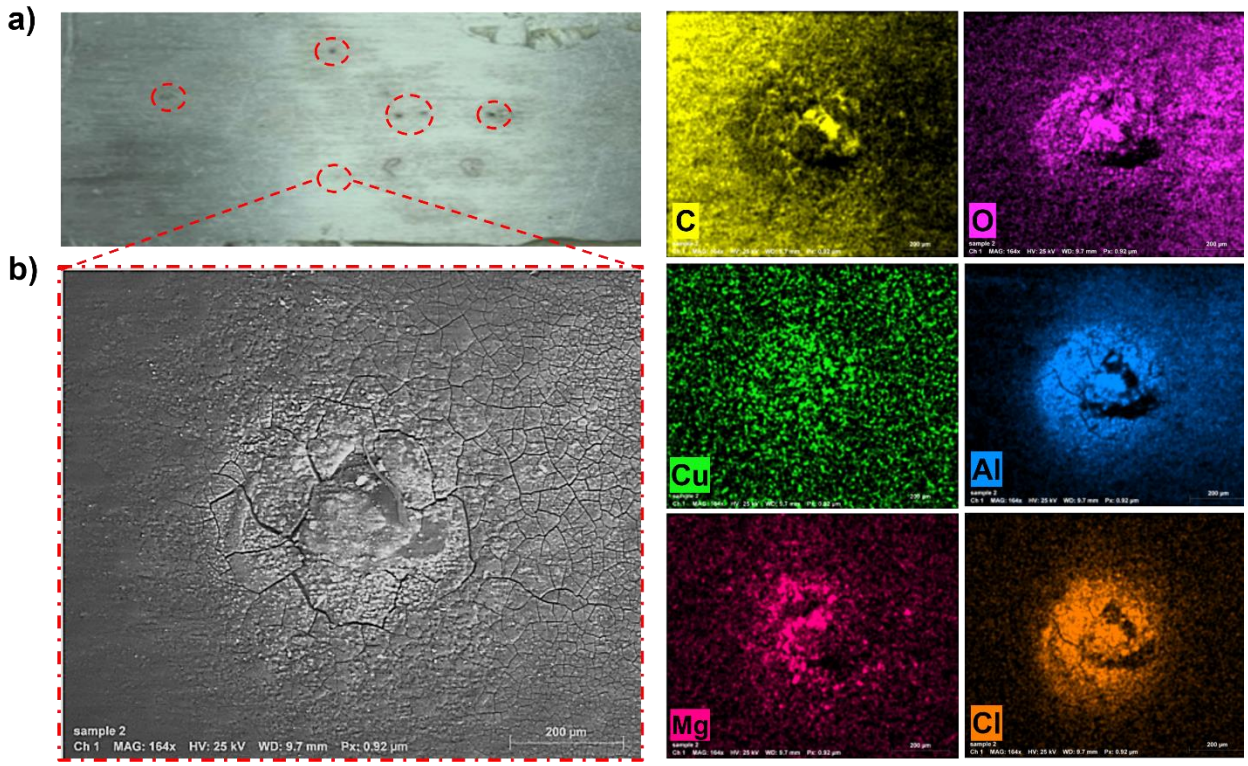

Figure S5. Optical image of epoxy coated AA2024 (a) and EDX mapping of the pitting corrosion after 25 days immersion (b). Color mapping: C – yellow, O – purple, Cu – light green, Al – blue, Mg – pink, Cl – orange.

- Coating delamination in the MOF/epoxy coating:

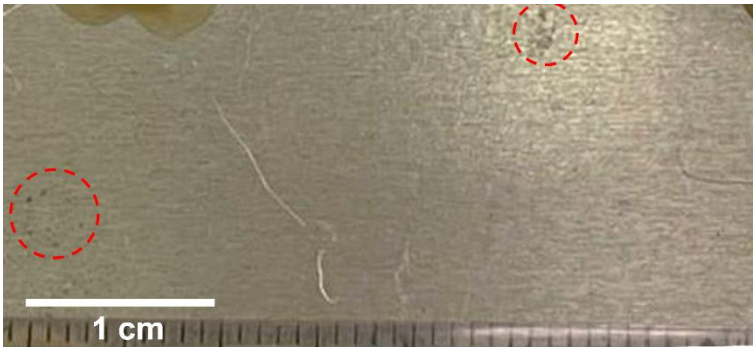

Figure S6. Optical images of the MOF/epoxy coated AA2024 samples after 65 days of immersion in 3.5%NaCl, showing slight coating delamination at the marked spots (red circles).

- Contact angle measurement:

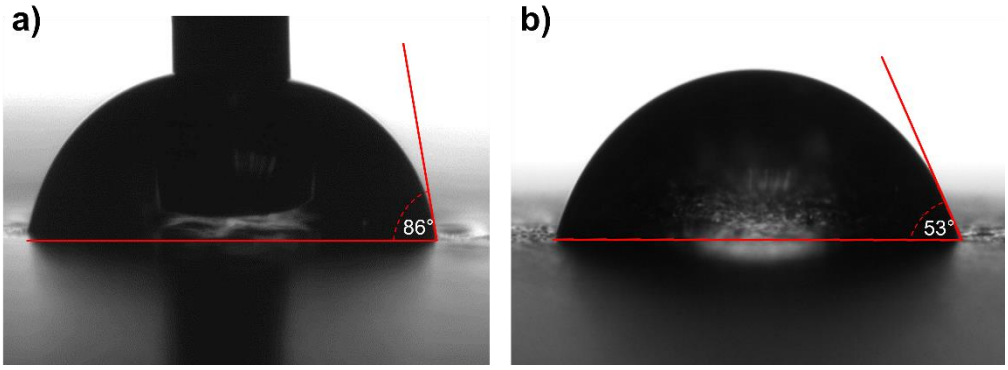

Figure S7. Optical images of the contact angle measurements of (a) epoxy (b) MOF/epoxy coatings.

References

[1] S. Biswas, D. E. P. Vanpoucke, T. Verstraelen, M. Vandichel, S. Couck, K. Leus, Y.-Y. Liu, M. Waroquier, V. Van Speybroeck, J. F. M. Denayer, and P. Van Der Voort, "New Functionalized Metal–Organic Frameworks MIL-47-X (X = −Cl, −Br, −CH3, −CF3, −OH, −OCH3): Synthesis, Characterization, and CO2 Adsorption Properties," *The Journal of Physical Chemistry C,* vol. 117, no. 44, pp. 22784-22796, 2013, doi: https://doi.org/10.1021/jp406835n.

[2] K. Barthelet, J. Marrot, D. Riou, and G. Férey, "A Breathing Hybrid Organic–Inorganic Solid with Very Large Pores and High Magnetic Characteristics," *Angewandte Chemie International Edition,* vol. 41, no. 2, pp. 281-284, 2002, doi: https://doi.org/10.1002/1521-3773(20020118)41:2<281::AID-ANIE281>3.0.CO;2-Y.

[3] A. E. J. Hoffman, L. Vanduyfhuys, I. Nevjestić, J. Wieme, S. M. J. Rogge, H. Depauw, P. Van Der Voort, H. Vrielinck, and V. Van Speybroeck, "Elucidating the Vibrational Fingerprint of the Flexible Metal–Organic Framework MIL-53(Al) Using a Combined Experimental/Computational Approach," *The Journal of Physical Chemistry C,* vol. 122, no. 5, pp. 2734-2746, 2018, doi: https://doi.org/10.1021/acs.jpcc.7b11031.

[4] H. Zhang, X. Xiao, X. Lu, G. Chai, Y. Sun, Y. Zhan, and G. Xu, "A cost-effective method to fabricate VO2 (M) nanoparticles and films with excellent thermochromic properties," *Journal of Alloys and Compounds,* vol. 636, pp. 106-112, 2015, doi: https://doi.org/10.1016/j.jallcom.2015.01.277.

[5] D. Surya Bhaskaram, R. Cheruku, and G. Govindaraj, "Reduced graphene oxide wrapped V2O5 nanoparticles: green synthesis and electrical properties," *Journal of Materials Science: Materials in Electronics,* vol. 27, no. 10, pp. 10855-10863, 2016, doi: https://doi.org/10.1007/s10854-016-5194-x.

[6] C. O'Dwyer, V. Lavayen, S. B. Newcomb, M. A. Santa Ana, E. Benavente, G. Gonzalez, and C. S. Torres, "Vanadate conformation variations in vanadium pentoxide nanostructures," *Journal of the Electrochemical Society,* vol. 154, no. 8, p. K29, 2007, doi: https://doi.org/10.1149/1.2746556.

[7] T. Loiseau, C. Serre, C. Huguenard, G. Fink, F. Taulelle, M. Henry, T. Bataille, and G. Férey, "A Rationale for the Large Breathing of the Porous Aluminum Terephthalate (MIL-53) Upon Hydration," *Chemistry – A European Journal,* vol. 10, no. 6, pp. 1373-1382, 2004, doi: https://doi.org/10.1002/chem.200305413.

[8] C. L. Londoño-Calderón, C. Vargas-Hernández, and J. F. Jurado, "Desorption influence of water on structural, electrical properties and molecular order of vanadium pentoxide xerogel films," *Revista mexicana de física,* vol. 56, pp. 411-415, 2010. [Online]. Available: http://www.scielo.org.mx/scielo.php?script=sci_arttext&pid=S0035-001X2010000500009&nrm=iso.

[9] P. G. Yot, Q. Ma, J. Haines, Q. Yang, A. Ghoufi, T. Devic, C. Serre, V. Dmitriev, G. Férey, C. Zhong, and G. Maurin, "Large breathing of the MOF MIL-47(VIV) under mechanical pressure: a joint experimental–modelling exploration," *Chemical Science,* vol. 3, no. 4, pp. 1100-1104, 2012, doi: https://doi.org/10.1039/C2SC00745B.